

---

**MAGNETISM  
AND FERROELECTRICITY**

---

## Studies of the Thermodynamic Properties of the Ordered Perovskites $\text{Pb}_2\text{CdWO}_6$ and $\text{Pb}_2\text{YbTaO}_6$ within a Broad Temperature Range

**M. V. Gorev\*, I. N. Flerov\*, V. S. Bondarev\*, and Ph. Sciau\*\***

\* *Kirenskiĭ Institute of Physics, Siberian Division, Russian Academy of Sciences,  
Akademgorodok, Krasnoyarsk, 660036 Russia*

*e-mail: gorev@iph.krasn.ru*

\*\* *CEMEC-CNRS, 31055 Toulouse, France*

Received June 26, 2001

**Abstract**—This paper reports on measurements of the specific heat of  $\text{Pb}_2\text{CdWO}_6$  made at temperatures ranging from 80 to 750 K and of  $\text{Pb}_2\text{YbTaO}_6$  within the 350- to 700-K temperature range. First-order phase transitions from the cubic phase at 677.3 and 581 K, respectively, were observed, and their thermodynamic characteristics were determined. The entropy change on the phase transitions is close to  $R\ln 4$  for both compounds. The results obtained are discussed in terms of the model of position disordering of the lead ions. It was established that below 350 K,  $\text{Pb}_2\text{CdWO}_6$  can exist in two states, stable and metastable, depending on the sample thermal prehistory. © 2002 MAIK “Nauka/Interperiodica”.

Many perovskite-like oxygen compounds with a three-dimensional framework of corner-sharing octahedra undergo various sequences of phase transitions with decreasing temperature which entail the formation of a superstructure; however, only in some of them have incommensurate modulated structures been revealed. Only a few such compounds are thus far known to exist among the  $\text{Pb}_2B'B''\text{O}_6$  mixed perovskites, in particular,  $\text{Pb}_2\text{ScTaO}_6$  [1],  $\text{Pb}_2\text{CoWO}_6$  [2, 3],  $\text{Pb}_2\text{CdWO}_6$  [4], and, possibly,  $\text{Pb}_2\text{YbTaO}_6$  [5, 6]. The reasons for the incommensurate phase formation and the phase transitions of this type remain poorly studied.

This paper presents the results of a study on the specific heat of two ordered perovskites,  $\text{Pb}_2\text{CdWO}_6$  and  $\text{Pb}_2\text{YbTaO}_6$ , carried out within a broad temperature range with the purpose of determining the thermodynamic parameters of the phase transitions and the behavior of these compounds in the temperature regions where anomalies in the dielectric properties are observed.

The occurrence of the antiferroelectric-II–antiferroelectric-I and antiferroelectric-I–paraelectric cubic phase transitions (at 370 and 683 K, respectively) in  $\text{Pb}_2\text{CdWO}_6$  was first reported in [7], with the lower temperature phase found to be pseudomonoclinic. In a later x-ray study [4], only one phase transition, at 683 K, was detected; in contrast to [7], no appreciable changes in the unit-cell parameters were observed to occur near 370 K. In the higher temperature phase, the compound has an fcc structure  $Fm\bar{3}m$  ( $Z = 4$ ), which is characteristic of ordered mixed perovskites. Below the phase-transition point, the x-ray diffractograms were

interpreted as corresponding to a pseudoorthorhombic unit cell [ $a_0 = a_c$ ,  $b_0 = (b_c + c_c)/2$ ,  $c_0 = (b_c - c_c)/2$ ] similar to the unit cell of the lower temperature phase of  $\text{Pb}_2\text{CoWO}_6$  [3, 8]. In this phase, one observes additional weak reflections, which were assigned in [4] to incommensurate distortions.

The  $\text{Pb}_2\text{YbTaO}_6$  compound was also reported [5, 6, 9] to undergo two phase transitions which proceed in the following sequence: cubic paraelectric ( $Fm\bar{3}m$ )–antiferroelectric at  $T_1 = 558$  K and antiferroelectric–ferroelectric ( $Pcm2_1?$ ) at  $T_2 \approx 450$  K. The anomaly in the dielectric permittivity at  $T_2$  is very weak, and noticeable dispersion is observed.

The samples for investigation were prepared through solid-state synthesis from a stoichiometric mixture of the starting oxides. The mixture was heated in a gold ampule and kept at a high temperature for several hours. The quality and purity of the samples were verified on a Siemens-D-5000 x-ray diffractometer. A diffractometric analysis showed the sample to contain neither the starting substances used in the solid-state synthesis nor foreign phases [4]. It was also established that there is no disorder in the distribution of the  $\text{Cd}^{2+}$  and  $\text{W}^{6+}$  ions, nor in the  $\text{Yb}^{3+}$  and  $\text{Ta}^{5+}$  ions occupying positions at the centers of the corresponding octahedra [4].

The heat capacity of  $\text{Pb}_2\text{CdWO}_6$  was measured in the 80- to 370-K temperature range with an adiabatic calorimeter in the discrete and continuous heating modes. The powder sample, 4.297 g in mass, employed earlier in structure refinement measurements [4], was

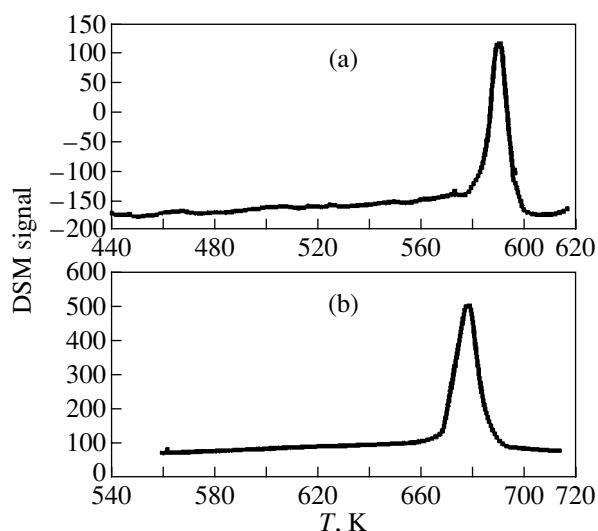


**Fig. 1.** DSM-2M microcalorimetric traces obtained on (a)  $\text{Pb}_2\text{CdWO}_6$  and (b)  $\text{Pb}_2\text{YbTaO}_6$ .

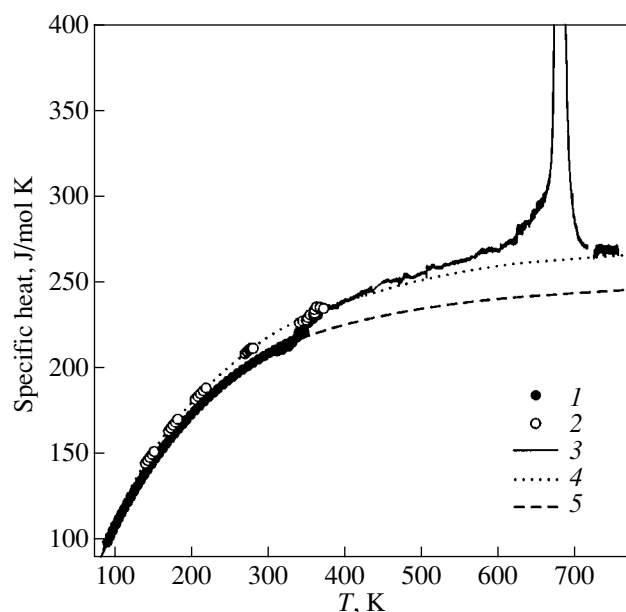


**Fig. 2.** Specific heat of  $\text{Pb}_2\text{CdWO}_6$  measured within a broad temperature range: (1) first series of measurements; (2) the second series and subsequent measurements; (3) DSM measurements made at high temperatures; and (4, 5) lattice specific heat.

placed in an indium container which was sealed in a helium environment. The container heat capacity was measured in a separate experiment. The scatter of experimental points from a smoothed curve did not exceed 0.5%.

In the 330- to 770-K range, the heat capacities of  $\text{Pb}_2\text{CdWO}_6$  and  $\text{Pb}_2\text{YbTaO}_6$  were measured with a dif-

ferential scanning microcalorimeter on a computerized DSM-2M setup. The samples were 0.588 and 0.410 g in mass, respectively. The error inherent in this method (~5%) is substantially larger than that in an adiabatic calorimeter.

The results obtained on samples of  $\text{Pb}_2\text{CdWO}_6$  and  $\text{Pb}_2\text{YbTaO}_6$  with the differential scanning microcalorimeter are presented in Fig. 1.  $\text{Pb}_2\text{CdWO}_6$  exhibited only one noticeable anomaly, with a maximum at 677 K (Fig. 1a). In  $\text{Pb}_2\text{YbTaO}_6$ , the anomaly is observed at 581 K (Fig. 1b). Neither of the crystals revealed any substantial anomalies in the temperature regions where structural changes were reported in [5, 7, 9] to take place. This is possibly associated with the insufficiently high sensitivity of the DSM method and the smallness of the thermal effect of this phase transition in  $\text{Pb}_2\text{YbTaO}_6$ , a factor pointed out in [5]. The enthalpy changes at the high-temperature phase transitions in  $\text{Pb}_2\text{CdWO}_6$  and  $\text{Pb}_2\text{YbTaO}_6$  were found to be  $6800 \pm 300$  and  $6250 \pm 350$  J/mol, respectively.

Figure 2 displays the results obtained in a study of the heat capacity of  $\text{Pb}_2\text{CdWO}_6$ . The specific heat does not exhibit anomalous behavior up to 330 K. When heated above 330 K, the sample reveals a stepwise increase in the specific heat by ~5% within a narrow (~10 K) temperature range (curve 1 in Fig. 2). The values of the low-temperature specific heat obtained in repeated measurements were found to be higher than those obtained in the first series. No changes in  $C_p(T)$  near 330 K were presently found (curve 2 in Fig. 2). The two levels of the specific heat obtained in different series of measurements below this temperature imply that a sample can reside in two possible states. Attempts were made to act on the state of the sample through thermal cycling and by maintaining it at liquid-nitrogen and room temperature for 14 days. Subsequent measurements showed, however, that this does not restore the specific heat to its original value of below 330 K. It may be conjectured that the equilibrium state corresponding to the lower value of the specific heat is reached as a result of aging, which is caused by prolonged storage of the sample at room temperature. Effects of aging, which influence the behavior of the dielectric properties in perovskite-like compounds, were reported in [10]. In our case, the sample was maintained at room temperature for several years before the beginning of the calorimetric measurements. The nonequilibrium state may have arisen after the sample was heated above 330 K (above the temperature of storage) and have persisted under subsequent cooling. To investigate this phenomenon, we will repeat the specific-heat measurements made on the same sample following prolonged (about a year) storage at room temperature.

The anomaly of the specific heat associated with the phase transition from the cubic phase is observed in scanning-microcalorimeter measurements at 677.3 K

(curve 3 in Fig. 2), which is slightly lower than the value quoted in [4].

The results of the first series of measurements below 320 K and of the repeated experiment with the adiabatic calorimeter from 140 to 360 K were treated using a combination of the Debye and Einstein functions:

$$C_L(T) = A \left( \frac{T}{\Theta_D} \right)^3 \int_0^{\frac{\Theta_D}{T}} x^4 \frac{\exp(x)}{(\exp(x) - 1)^2} dx + B \left( \frac{\Theta_E}{T} \right)^2 \frac{\exp\left(\frac{\Theta_E}{T}\right)}{\left(\exp\left(\frac{\Theta_E}{T}\right) - 1\right)^2}. \quad (1)$$

The relations derived in this treatment are plotted in Fig. 2 (curves 4, 5). Extrapolation of the relation obtained in the repeated series of measurements to the high-temperature region reveals good agreement with the data obtained from scanning microcalorimetry above the phase-transition temperature. In our opinion, this observation, as well as the good fit of the data in the temperature range near 370–400 K, is evidence of a fairly good agreement between the results obtained with the two experimental methods and provides grounds for their combined treatment.

It should be pointed out that when extrapolated to the high-temperature domain, the specific heat [described by Eq. (1)] derived from the original experiments in the 80- to 320-K range tends to the classical value following from the Dulong–Petit law. The values of the specific heat found at high temperatures in the second series of measurements lie above this level. The reason for this remains unclear. We stress once more that DSM measurements of the specific heat are made with an error of about 5%. The systematic error can increase at high temperatures.

The anomalous specific heat associated with the phase transition from the cubic phase is observed in  $\text{Pb}_2\text{CdWO}_6$  within a fairly broad temperature range, as wide as  $\sim 150$  K below the transition temperature and  $\sim 15$ – $20$  K above it. The integrated thermodynamic characteristics of the phase transition were derived from the anomalous part of the specific heat  $\Delta C_p(T) = C_p(T) - C_L(T)$ , where, for the lattice specific heat  $C_L(T)$ , we used results obtained by fitting the low-temperature specific heat with Eq. (1). The phase-transition specific enthalpy  $\Delta H = \int \Delta C_p(T) dT$  is  $7320 \pm 360$  J/mol, which slightly exceeds the value extracted from the DSM measurements themselves ( $6800 \pm 300$  J/mol). The specific entropy of the phase transition, calculated by integrating the  $\Delta C_p(T)/T$  function, is plotted in Fig. 3. The total change in the specific entropy is  $\Delta S = 11.1 \pm 0.6$  J/mol K  $\approx 1.33R$ . Also shown in Fig. 3 is the change in the specific entropy of  $\text{Pb}_2\text{YbTaO}_6$ ,  $\Delta S = 10.9 \pm$

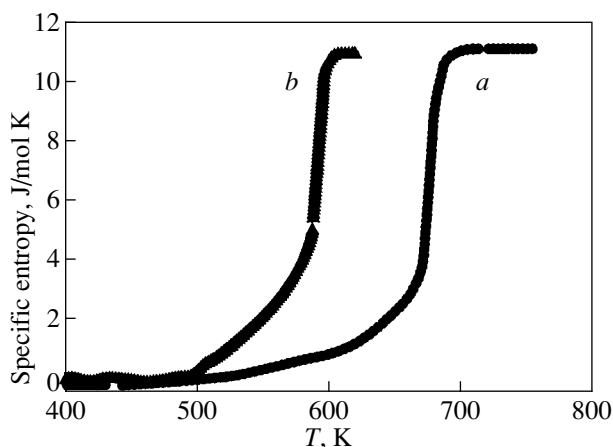


Fig. 3. Temperature dependence of the excess specific entropy: *a*— $\text{Pb}_2\text{CdWO}_6$  and *b*— $\text{Pb}_2\text{YbTaO}_6$ .

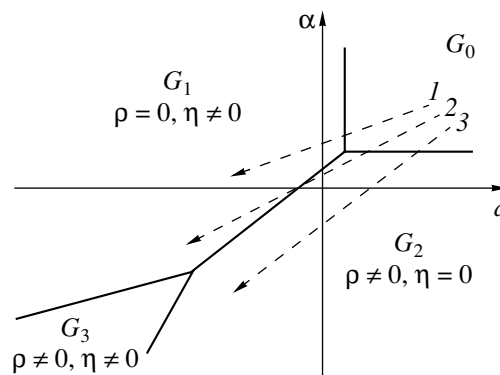


Fig. 4. Phase diagram constructed on the  $\alpha$ - $a$  plane in the model of [15, 16].  $G_0(Fm\bar{3}m)$  is the praphase,  $G_1$  is a commensurate phase, and  $G_2$  and  $G_3$  are incommensurate phases.

0.6 J/mol K, which was derived from the DSM measurements.

The value of  $\Delta S$  obtained in this work for both compounds is large and close to  $R \ln 4$ , which is in accordance with our earlier data on the related compounds  $\text{Pb}_2\text{CoWO}_6$  and  $\text{Pb}_2\text{MgWO}_6$ , which also undergo transitions from the cubic to a pseudoorthorhombic phase [11, 12]. Such a large change in the entropy indicates a substantial role being played by ordering processes in the phase-transition mechanism.

Judging from structural data on the  $\text{Pb}_2B'B''\text{O}_6$  ordered perovskites [13, 14], Pb ions have the largest temperature parameter in the cubic phase if we assume them to occupy the  $8c$  positions. In the distorted phase, this parameter is of normal magnitude if the phase is pseudoorthorhombic. This provided grounds for the assumption that lead ions in the cubic phase are positionally disordered [14]. There are three models of pos-

sible disorder which consider the lead-ion displacements from the  $8c$  position in the  $[100]$ -,  $[110]$ -, and  $[111]$ -type directions.

Symmetry considerations leave six equally probable positions for the lead ions in the first model, twelve in the second, and four in the third. A refinement of the  $\text{Pb}_2\text{CoWO}_6$  and  $\text{Pb}_2\text{MgWO}_6$  structures made within these models yields the following results [13, 14]. The lowest value of the  $R$  factor for  $\text{Pb}_2\text{CoWO}_6$  was obtained in the case of lead disordered over twelve positions (the  $[110]$  model). For  $\text{Pb}_2\text{MgWO}_6$ , all the models considered yielded very close values of the  $R$  factor, making it difficult to give preference to any one of them. In the distorted phase, the lead ions are displaced primarily along the  $[100]$ -type directions of the pseudocubic unit cell. This may occur as a result of complete lead-atom ordering in the  $[100]$  model and should be accompanied by an entropy change  $\Delta S = 2R\ln 6 = R\ln 36$ . In the  $[110]$  model, the lead should remain partially disordered over two or four positions in the distorted phase in order to provide the experimentally observed mean displacements. The specific entropy is changed in this case by  $\Delta S = 2R\ln(12/4) = R\ln 9$  or  $2R\ln(12/2) = R\ln 36$ . In the  $[111]$  model, only two of the four possible lead-ion positions should remain in the distorted phase, thus changing the entropy by  $\Delta S = 2R\ln(4/2) = R\ln 4$ .

The values of  $\Delta S$  determined by us agree only with the  $[111]$  model; the entropy changes calculated within the other models far exceed those observed in all the  $\text{Pb}_2B'B''\text{O}_6$  compounds studied in this work and in [11, 12].

Some  $\text{Pb}_2B'B''\text{O}_6$  compounds revealed soft modes in the inelastic neutron and Raman scattering spectra [15, 16]. One may thus conjecture that the phase-transition mechanism in these compounds involves both lead ordering and oxygen-atom displacements. Processes of the first kind provide the major contribution to the entropy change. That the values of  $\Delta S$  found in all the compounds studied are close to  $R\ln 4$  suggests the same lead-disordering type to be operative in the cubic phase.

Studies of the  $\text{Pb}_2\text{CoWO}_6$  compound suggest a phenomenological model of phase transitions to incommensurate and commensurate phases [17]. It was proposed in [17] that an incommensurate phase arises at  $T_1$  as a result of soft mode condensation at the point  $k_1 = (k_x, k_x, 2\pi/a)$  in the Brillouin zone. At  $T_2$ , additional x-ray reflections appear, which correspond to the wave vector  $k_2 = (0, 0, 2\pi/a)$  (the  $X$  point of the Brillouin zone). Reflections of the two types coexist within a broad ( $\sim 100$  K wide) temperature region. The thermodynamic potential has the form [17]

$$F = \frac{\alpha}{2}\rho^2 + \frac{\beta}{4}\rho^4 + \frac{a}{2}(\eta_1^2 + \eta_3^2) + \frac{b_1}{4}(\eta_1^4 + \eta_3^4) + \frac{b_2}{2}\eta_1^2\eta_3^2 + \frac{c}{6}(\eta_1^6 + \eta_3^6) + \delta\rho^2(\eta_1^2 + \eta_3^2), \quad (2)$$

where  $\rho$  is the magnitude of the order parameter of the incommensurate phase and  $\eta_1$  and  $\eta_3$  are the nonzero components of the order parameter corresponding to the ferroelectric phase. The coefficient  $\delta$  describes the interaction of the two order parameters. To include the possibility of first-order transitions associated with these two order parameters, one has to add a term of the sixth power in  $\rho$  to the potential in Eq. (2) [18]. Depending on the actual values of the coefficients of the potential in Eq. (2), one may conceive various sequences of phase transitions: cubic paraelectric  $G_0 \rightarrow$  commensurate  $G_1$  ( $\rho = 0, \eta \neq 0$ ), cubic  $G_0 \rightarrow$  incommensurate  $G_2$  ( $\rho \neq 0, \eta = 0$ ), and cubic  $G_0 \rightarrow$  incommensurate  $G_2$  ( $\rho \neq 0, \eta = 0$ )  $\rightarrow$  incommensurate  $G_3$  ( $\rho \neq 0, \eta \neq 0$ )  $\rightarrow$  commensurate  $G_1$  ( $\rho = 0, \eta \neq 0$ ). The thermodynamic paths for these transition sequences are shown in Fig. 4 in a schematic phase diagram in  $\alpha$ - $a$  coordinates (the thermodynamic-potential parameters) by lines 1, 2, and 3, respectively. The first sequence is likely to be realized in  $\text{Pb}_2\text{MgWO}_6$ , where one phase transition to the commensurate phase  $G_1$  is observed [14]. In  $\text{Pb}_2\text{CoWO}_6$  with a larger cation, the intermediate incommensurate phase  $G_2$  becomes stable in the 258- to 304-K temperature range. In  $\text{Pb}_2\text{CdWO}_6$ , with a still larger cation, the region of stability of the intermediate incommensurate phase  $G_2$  broadens and, according to our studies, no transition to the  $G_1$  or  $G_3$  phase occurs, at least down to 80 K. As for  $\text{Pb}_2\text{YbTaO}_6$ , the above phase diagram is also applicable to description of the phase-transition sequences in this compound, because, as reported in [5], its intermediate phase is incommensurate.

## ACKNOWLEDGMENTS

This study was supported by the Russian Foundation for Basic Research, project no. 00-15-96790.

## REFERENCES

1. C. A. Randall, S. A. Markgraf, A. S. Bhalla, and K. Baba-Kishi, *Phys. Rev. B* **40**, 413 (1989).
2. H. Tamura, *Ferroelectrics* **21**, 449 (1978).
3. Ph. Sciau, K. Krusche, P. A. Buffat, and H. Schmid, *Ferroelectrics* **107**, 235 (1990).
4. Ph. Sciau and D. Graille, in *Aperiodic'94*, Ed. by G. Chapuis and W. Paciorek (World Scientific, Singapore, 1995), pp. 460–464.
5. E. S. Gagarina, V. V. Demidova, V. V. Eremkin, *et al.*, *Kristallografiya* **44** (2), 281 (1999) [*Crystallogr. Rep.* **44**, 247 (1999)].
6. N. Yasuda and J. Konda, *Ferroelectrics* **158**, 405 (1994).
7. Yu. V. Roginskaya and Yu. N. Venetsev, *Kristallografiya* **10** (3), 341 (1965) [*Sov. Phys. Crystallogr.* **10**, 275 (1965)].

8. G. Baldinozzi, Ph. Sciau, and P. A. Buffat, *Solid State Commun.* **86** (9), 541 (1993).
9. V. A. Isupov and N. N. Kraĭnik, *Fiz. Tverd. Tela (Leningrad)* **6**, 3713 (1964) [*Sov. Phys. Solid State* **6**, 2975 (1964)].
10. H. Fan, L. Zhang, and X. Yao, *J. Phys.: Condens. Matter* **12**, 4381 (2000).
11. I. N. Flerov, M. V. Gorev, and Ph. Sciau, *Fiz. Tverd. Tela (St. Petersburg)* **41** (9), 1686 (1999) [*Phys. Solid State* **41**, 1544 (1999)].
12. I. N. Flerov, M. V. Gorev, and Ph. Sciau, *J. Phys.: Condens. Matter* **12** (5), 559 (2000).
13. G. Baldinozzi, Ph. Sciau, and J. Lapasset, *Phys. Status Solidi A* **133** (1), 17 (1992).
14. G. Baldinozzi, Ph. Sciau, M. Pinot, and D. Graille, *Acta Crystallogr. B* **51**, 668 (1995).
15. G. Baldinozzi, Ph. Sciau, and A. Bulou, *J. Phys.: Condens. Matter* **7**, 8109 (1995).
16. W. Bührer, W. Brixel, and H. Schmid, in *Phonons 85* (World Scientific, Singapore, 1985), p. 325.
17. F. Maaroufi, P. Toledano, H. Schmid, *et al.*, *Ferroelectrics* **79**, 295 (1988).
18. Yu. M. Gufman and E. S. Larkin, *Fiz. Tverd. Tela (Leningrad)* **22** (2), 463 (1980) [*Sov. Phys. Solid State* **22**, 270 (1980)].

*Translated by G. Skrebtsov*